Journal of Virology, Oct. 2010, p. 9831–9839 Vol. 84, No. 19
0022-538X/10/$12.00 doi:10.1128/JVI.01163-10

A Novel Model of Lethal Hendra Virus Infection in African Green Monkeys and the Effectiveness of Ribavirin Treatment▽

Barry Rockx,[1] Katharine N. Bossart,[3,4] Friederike Feldmann,[1] Joan B. Geisbert,[3,5,6] Andrew C. Hickey,[7]† Douglas Brining,[2] Julie Callison,[1] David Safronetz,[1] Andrea Marzi,[1] Lisa Kercher,[2] Dan Long,[2] Christopher C. Broder,[7] Heinz Feldmann,[1]* and Thomas W. Geisbert[3,4,5,6]*

Laboratory of Virology[1] and Rocky Mountain Veterinary Branch,[2] Division of Intramural Research, National Institute of Allergy and Infectious Diseases, National Institutes of Health, 903 S. 4th Street, Hamilton, Montana; National Emerging Infectious Diseases Laboratories Institute[3] and Department of Microbiology,[4] Boston University School of Medicine, 620 Albany Street, Boston, Massachusetts; Galveston National Laboratory[5] and Department of Microbiology and Immunology,[6] University of Texas Medical Branch, 301 University Blvd., Galveston, Texas; and Department of Microbiology and Immunology, Uniformed Services University of the Health Sciences, 4301 Jones Bridge Road, Bethesda, Maryland[7]

Received 31 May 2010/Accepted 2 July 2010

The henipaviruses, Hendra virus (HeV) and Nipah virus (NiV), are emerging zoonotic paramyxoviruses that can cause severe and often lethal neurologic and/or respiratory disease in a wide variety of mammalian hosts, including humans. There are presently no licensed vaccines or treatment options approved for human or veterinarian use. Guinea pigs, hamsters, cats, and ferrets, have been evaluated as animal models of human HeV infection, but studies in nonhuman primates (NHP) have not been reported, and the development and approval of any vaccine or antiviral for human use will likely require efficacy studies in an NHP model. Here, we examined the pathogenesis of HeV in the African green monkey (AGM) following intratracheal inoculation. Exposure of AGMs to HeV produced a uniformly lethal infection, and the observed clinical signs and pathology were highly consistent with HeV-mediated disease seen in humans. Ribavirin has been used to treat patients infected with either HeV or NiV; however, its utility in improving outcome remains, at best, uncertain. We examined the antiviral effect of ribavirin in a cohort of nine AGMs before or after exposure to HeV. Ribavirin treatment delayed disease onset by 1 to 2 days, with no significant benefit for disease progression and outcome. Together our findings introduce a new disease model of acute HeV infection suitable for testing antiviral strategies and also demonstrate that, while ribavirin may have some antiviral activity against the henipaviruses, its use as an effective standalone therapy for HeV infection is questionable.

Hendra virus (HeV) and Nipah virus (NiV) are members of the genus *Henipavirus* (family *Paramyxoviridae*) that can cause severe respiratory illness and/or encephalitis in a wide variety of mammals, including horses, pigs, and humans (7, 23). HeV was identified as the causative agent of an acute respiratory disease in horses in 1994 in Queensland, Australia (23), and to date there have been 14 outbreaks in Australia since, with at least one occurrence per year since 2006, most recently in May 2010 (ProMed-mail no. 20100522.1699 [International Society for Infectious Diseases, http://www.promedmail.org]). Every outbreak of HeV has involved horses as the initial infected host, and there have been a total of seven human cases arising from exposure to infected horses. Four human fatalities have occurred (22), with the most recent occurring in August of 2009 (ProMed-mail no. 20090826.2998 and 20090903.3098). All patients initially presented with influenza-like illnesses (ILIs) after an incubation period of 7 to 16 days. While two individuals recovered from ILI, one patient developed pneumonitis and died from multiorgan failure. Three of the lethal cases developed encephalitic manifestations (mild confusion and ataxia), with two patients experiencing seizures (22, 23, 27).

Data on the histopathology of fatal human HeV cases are limited, but the pathology includes small necrotic plaques in the cerebrum and cerebellum, in addition to mild parenchymal inflammation (21, 27). Severe parenchymal inflammation and necrosis were observed in the lungs. More extensive histopathologic data are available from 32 autopsies of fatal human NiV cases (28). Similarly to the HeV cases, pathology was characterized by systemic vasculitis and parenchymal necrosis in the central nervous system (CNS), while in the lung, pathological findings mainly included vasculitis, fibrinoid necrosis, alveolar hemorrhage, pulmonary edema, and aspiration pneumonia. Other organs that were affected included heart, kidney, and spleen and showed generally mild or focal inflammation. The development of syncytial multinucleated endothelial cells is characteristic of both HeV and NiV (27, 28). At present, the

* Corresponding author. Mailing address for T. W. Geisbert: Galveston National Laboratory and Department of Microbiology and Immunology, University of Texas Medical Branch, 301 University Blvd., Galveston, TX 77555. Phone: (409) 266-6906. Fax: (409) 772-2366. E-mail: tom.geisbert@utmb.edu. Mailing address for H. Feldmann: Laboratory of Virology, Division of Intramural Research, National Institute of Allergy and Infectious Diseases, National Institutes of Health, 903 S. 4th Street, Hamilton, MT 59840. Phone: (406) 375-7410. Fax: (406) 375-7416. E-mail: feldmannh@niaid.nih.gov.

† Present address: National Emerging Infectious Diseases Laboratories Institute and Department of Microbiology, Boston University School of Medicine, 620 Albany Street, Boston, MA 02118.

▽ Published ahead of print on 21 July 2010.

details of the pathogenesis and histopathological changes mediated by either HeV or NiV infection in humans are naturally derived from only the late phases of the disease course, and therefore a relevant animal model is needed that mimics the disease progression seen in humans.

Pteropid fruit bats, commonly known as flying foxes in the family *Pteropodidae*, are the principle natural reservoirs for both NiV and HeV (reviewed in reference 3). However, these henipaviruses display a broad species tropism, and in addition to bats, horses and humans, natural and/or experimental infection of HeV has been demonstrated in guinea pigs, hamsters, pigs, cats, and ferrets (25). Experimental infections of Syrian hamsters with HeV is lethal, and animals show disease similar to that of human cases, including respiratory and neurological symptoms, depending on the dose (11; unpublished data). In this model, viral RNA can be detected in various organs of infected hamsters, including brain, lung, kidney, heart, liver, and spleen. The main histopathological findings included parenchymal infection in various organs, including the brain, with vasculitis and syncytial multinucleated endothelial cells in many blood vessels (11). While this model is useful in studying pathogenesis, it is limited in the availability of reagents to do so.

There are currently no vaccines or treatments licensed for human use. Several *in vitro* studies have shown that ribavirin is effective against both HeV and NiV infection (1, 2, 29). An open-label ribavirin treatment trial was run during an outbreak of NiV in Malaysia in 1998 and reported to reduce mortality by 36% (6). Of the seven recorded human HeV cases, three patients were treated with ribavirin, one of whom survived (22). In the most recent outbreak of HeV in Australia, three additional people received ribavirin treatment in combination with chloroquine after suspected exposure to HeV-contaminated secretions from infected horses. While all three individuals survived, infection was not confirmed, and therefore it remains unknown whether the treatment had any beneficiary effect (ProMed-mail no. 20090826.2998). In addition, two animal studies in hamsters showed that ribavirin treatment delays but does not prevent death from NiV or HeV infection (8, 10). Therefore, an animal model with greater relevance to humans and that recapitulates the disease processes seen in human cases of HeV is needed to get a better answer to whether ribavirin might be effective against henipavirus infections. In addition, the U.S. FDA implemented the "Animal Efficacy Rule," which specifically applies to the development of therapeutic products when human efficacy studies are not possible or ethical, such as is often the case with highly virulent pathogens like HeV (24). Essentially, this rule allows for the evaluation of vaccines or therapeutics using data derived from studies carried out in at least two animal models. The licensure of any therapeutic modalities for HeV will require a thorough evaluation of HeV pathogenesis in nonhuman primates (NHPs).

In the present study, we report the development and characterization of a new nonhuman primate (NHP) model of lethal HeV infection in the African green monkey (AGM). The pathogenesis and disease progression in the AGM upon HeV infection essentially mirrored the lethal disease episodes seen among human cases of HeV. Using this new model, the efficacy of ribavirin treatment against lethal challenge with HeV was examined. Here we have shown that ribavirin treatment can significantly delay but not prevent death of AGMs from lethal HeV infection. In addition to severe respiratory symptoms in all animals, prolonged disease progression in ribavirin-treated animals was also marked by the appearance of neurological symptoms.

MATERIALS AND METHODS

Viruses and cells. HeV was kindly provided by the Special Pathogens Branch of the Centers for Disease Control and Prevention, Atlanta, GA. The virus was propagated on Vero E6 cells in Dulbecco's minimal essential medium (DMEM) supplemented with 10% fetal calf serum (HyClone, Logan, UT), L-glutamine, penicillin, and streptomycin at 37°C in a humidified CO_2 incubator (5%). Virus titration was performed using a 50% tissue culture infective dose ($TCID_{50}$) assay (tissue culture dose leading to 50% cytopathogenic effect) on 96-well plates (1×10^4 Vero E6 cells per well) with a 100-μl inoculum from 10-fold serial dilutions. Plates were incubated for 3 days at 37°C, and wells were scored for cytopathic effect (CPE). Virus concentrations were calculated as $TCID_{50}$/ml. All infectious work was performed in a class II biological safety cabinet in a biosafety level 4 (BSL4) laboratory at the Rocky Mountain Laboratories, Division of Intramural Research, National Institute of Allergy and Infectious Diseases, National Institutes of Health.

Animal infection. Twelve young adult African green monkeys (*Chlorocebus aethiops*), weighing 5 to 7 kg (Three Springs Scientific, Inc., PA) were caged individually. All animals were anesthetized by intramuscular injection of ketamine (10 to 15 mg/kg body weight) and inoculated intratracheally (i.t.) with 4×10^5 $TCID_{50}$ of HeV in 4 ml of DMEM on day 0. Nine animals were treated with ribavirin subcutaneously (s.c.), starting with a loading dose of 50 mg/kg under ketamine anesthesia, followed by a maintenance dose applied through s.c. injections of 10 mg/kg at 8-h intervals without anesthesia for 14 days or until animals were euthanized. Three animals were treated with ribavirin beginning 24 h prior to challenge, three animals received the initial ribavirin treatment beginning 12 h after challenge, and three other animals received the initial ribavirin treatment 48 h after challenge. The dose regimen for ribavirin was based on the experience with efficacy in NHPs for the treatment of Lassa fever virus infection (13). Animals were anesthetized for clinical examination, temperature, respiration rate, chest radiographs, blood draws, and swabs of nasal, oral, and rectal mucosa on days −7, −1, 0, 1, 3, 5, 7, 10, and 12 p.i. All animals were euthanized when clinical signs indicated terminal disease according to an endpoint scoring sheet. Upon necropsy, various tissues were collected for virological assays. Experiments were conducted under BSL4 conditions, and approval for animal experiments was obtained from the Institutional Animal Care and Use Committee. Animal work was performed by certified staff in an Association for Assessment and Accreditation of Laboratory Animal Care (AAALAC)-approved facility.

Sample collection. Nasal, oral, and rectal swabs were collected in 1 ml of Dulbecco's minimal essential medium (DMEM) (Sigma-Aldrich, St. Louis, MO) and vortexed for 30 s. Whole blood was collected in EDTA Vacutainers (Beckman Dickinson, Franklin Lakes, NJ). Immediately following sampling, 140 μl of blood or 140 μl DMEM from individual swab samples was added to 560 μl of AVL viral lysis buffer (Qiagen, Inc., Valencia, CA) for RNA extraction. For tissues, approximately 100 mg was stored in 1 ml RNAlater (Qiagen, Inc.) for 7 days to stabilize RNA. RNAlater was completely removed, and tissues were homogenized in 600 μl RLT buffer (Qiagen, Inc.) in a 2-ml cryovial using Qiagen tissue lyser and stainless steel beads. An aliquot representing approximately 30 mg was added to fresh RLT buffer (600-μl final volume) for RNA extraction. The tissues sampled include conjunctiva, tonsil, oro/nasopharynx, nasal mucosa, trachea, right bronchus, left bronchus, right lung upper lobe, right lung middle lobe, right lung lower lobe, right lung upper lobe, right lung middle lobe, right lung lower lobe, bronchial lymph node (LN), heart, liver, spleen, kidney, adrenal gland, pancreas, jejunum, colon transversum, brain (frontal and cerebellum), brain stem, cervical spinal cord, pituitary gland, mandibular LN, salivary LN, inguinal LN, axillary LN, mesenteric LN, urinary bladder, testes or ovaries, and femoral bone marrow. All blood samples and swabs were inactivated in AVL viral lysis buffer, and tissue samples were homogenized and inactivated in RLT buffer prior to removal from the BSL4 laboratory. Subsequently, RNA was isolated from blood and swabs using the QIAamp viral RNA kit (Qiagen, Inc.) and from tissues using the RNeasy minikit (Qiagen, Inc.) according to the manufacturer's instructions supplied with each kit.

HeV TaqMan PCR. The HeV TaqMan assay was developed using primers and probe that target the HeV nucleocapsid gene. The following HeV primers (high-performance liquid chromatography [HPLC] purified) from Integrated DNA

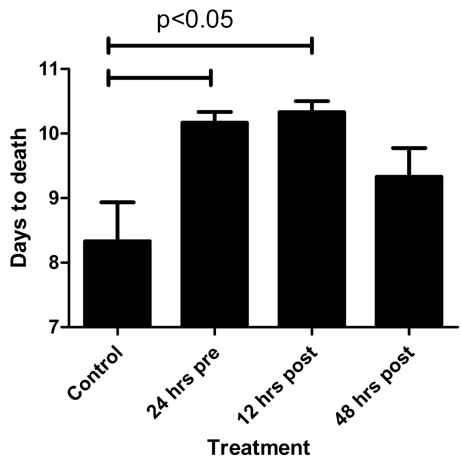

FIG. 1. Average time to death. Shown is the therapeutic effect of ribavirin treatment at 24 h prior to infection (pre) and 12 or 48 h postinfection on the time to death. Black bars represent average time to death for each group. Error bars represent the standard error of the mean of three animals.

Technologies (San Diego, CA) were used: H1487F (CAT CGG AAA GAA ACC CAC CTA A) and H1559 (GGT TTG GGT TCC TGG TCA TCT). The HeV probe (Applied Biosystems, Carlsbad, CA) primer H1511comp had the sequence 6-carboxyfluorescein (6FAM)-TCC TGA GTC TGC CTG AGG GCG GT-6-carboxytetramethylrhodamine (TAMRA). Ribosomal 18S primers and probe were used as an internal control. Primer and probe sequences for 18S have been described previously (18). One-step real-time PCR (RT-PCR) was done using Rotor-Gene multiplex RT-PCR kits (Qiagen, Inc.). All RT-PCR mixtures contained 2 μl of RNA. Master mixes were set up following the manufacturer's protocols with the following primer and probe concentrations: HeV, 1 μM H1487F, 1 μM H1559, and 0.25 μM H1511; 18S, 0.05 μM each primer and 0.2 μM probe. Each reaction was done in a total volume of 25 μl. HeV RNA extracted from the inoculum (10^5 $TCID_{50}$) was used as a positive control and as a standard curve for each assay. Standards and test samples were assayed in triplicate using the Rotor Gene 6000 detection system (Qiagen, Inc.) with the following parameters: 50°C for 10 min, 95°C for 5 min, and 40 cycles of 95°C for 5 s and 60°C for 10 s. Threshold cycle (C_T) values representing HeV nucleocapsid (N) gene expression were analyzed with Rotor Gene 6000 software, and data are shown as relative HeV N gene expression levels. For these data, a relative expression unit of 1 represents 4.7 $TCID_{50}$s of HeV inoculum.

Chest radiographs. A mobile digital radiography unit with a flat panel digital detector (Sound Technologies tru/Dr) and a portable X-ray generator (Poskom model PXP-HF) was used to acquire chest radiographs. The system operates on veterinary-specific software system (Vetpacs). Animals were positioned for ventral/dorsal radiography by using a Lexan V-shaped thoracic positioner. The radiographic views acquired included ventral/dorsa, right lateral, and left lateral thoracic images captured at peak inspiration while under anesthesia.

Hematology and blood biochemistry. Total white blood cell (WBC) count, lymphocyte, platelet, reticulocyte, and red blood cell counts, hemoglobin, hematocrit values, mean cell volume, mean corpsular volume and mean corpuscular hemoglobin concentrations were determined from EDTA-blood with the HemaVet 950FS+ laser-based hematology analyzer (Drew Scientific, Waterbury, CT). Serum biochemistry was analyzed from heparin-blood using the blood chemistry analyzer, iSTAT1 (Abbott Point of Care, Princeton, NJ). Using the EC8+ cartridge, blood urea nitrogen (BUN), glucose, chloride, sodium, potassium, hematocrit, hemoglobin, pH, partial CO_2 pressure (pCO_2), total CO_2 pressure (tCO_2), base excess (BEecf), and anion gap values were determined; creatinine values were evaluated using the Crea cartridges. Serum samples were tested for concentrations of albumin (ALB), amylase (AMY), alanine aminotransferase (ALT), aspartate aminotransferase (AST), alkaline phosphatase (ALP), gamma-glutamyltransferase (GGT), glucose (GLU), cholesterol (CHOL), total protein (TP), total bilirubin (TBIL), blood urea nitrogen (BUN), and creatinine (CRE) by using a Piccolo point-of-care blood analyzer (Abaxis, Sunnyvale, CA).

Virus titrations. Nasal, oral, and rectal swabs were collected and stored in 1 ml of Dulbecco's minimal essential medium (DMEM) and vortexed for 30 s. Whole blood was collected in EDTA Vacutainers. Tissue samples were weighed and homogenized in 10 equivalent volumes of DMEM to generate a 10% solution. The solution was centrifuged at 10,000 rpm under aerosol containment in a tabletop centrifuge for 5 min to pellet insoluble parts. All specimens were serially diluted in DMEM, and 100-μl volumes of each dilution were placed onto monolayers of Vero E6 cells in 96-well plates. Following a 3-day incubation at 37°C, the plates were scored for CPE and the $TCID_{50}$ was determined.

Histopathology and immunohistochemistry. A complete necropsy was performed on all animals. Tissue samples of all major organs were collected from each NHP for histopathologic and immunohistochemical examination and were immersion fixed in 10% neutral buffered formalin for at least 7 days under BSL4 conditions. Prior to removal from the BSL4 conditions, formalin was changed and specimens were processed under BSL2 conditions by conventional methods, embedded in paraffin, and underwent sectioning at a 5-μm thickness and hematoxylin and eosin or phosphotungstic acid-hematoxylin staining. Tissues for immunohistochemistry were stained on a Discovery XT automated stainer (Ventana Medical Systems) using an anti-Nipah virus nucleocapsid protein antibody

TABLE 1. Clinical scoring and outcome of HeV-infected African green monkeys untreated or treated with ribavirin

Treatment	Animal	Day of: Onset of symptoms	Day of: Euthanasia	Day of: Onset of neurological symptoms	Clinical sign(s)
Untreated (PBS)[a]	HeV1	5	7.5	NA[b]	Nasal discharge, labored breathing
	HeV6	6	8	NA	Nasal discharge
	HeV9	5	9.5	NA	Nasal discharge
Ribavirin					
24 h preinfection	HeV10	7	10	7	Nasal discharge, muscle fasciculations
	HeV11	6	10	NA	Nasal discharge, labored breathing
	HeV12	9	10.5	10	Nasal discharge, seizures
12 h p.i.	HeV3	5	10	9	Muscle fasciculations
	HeV4	5	10.5	9	Nasal discharge, muscle fasciculations
	HeV5	7	10.5	NA	Nasal discharge
48 h p.i.	HeV2	5	9.5	9	Nasal discharge, muscle fasciculations
	HeV7	5	10	9	Nasal discharge, muscle fasciculations, labored breathing
	HeV8	5	8.5	NA	Nasal discharge, labored breathing

[a] PBS, phosphate-buffered saline.
[b] NA, not applicable: no neurological symptoms were observed in these animals.

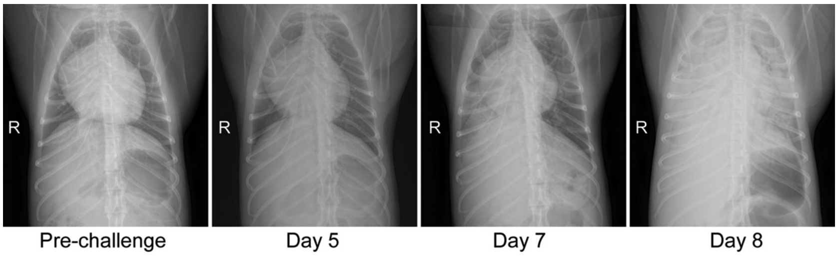

FIG. 2. Radiological and gross pathological changes in lungs of Hendra virus-infected African green monkeys. Radiologic progression of respiratory disease in animal HeV6 (Table 1), who was euthanized on day 8 due to severe respiratory distress. First evidence of congestion is observed on day 7 p.i., and infection rapidly progressed to diffuse interstitial infiltrates and pulmonary consolidation by day 8 p.i. R, right side.

(1:5,000) and the diaminobenzidine (DAB) map detection kit (Ventana Medical Systems) (18). Nonimmune rabbit IgG was used as a negative staining control.

RESULTS

Ribavirin treatment of Hendra virus-infected African green monkeys. Intratracheal inoculation of three untreated control animals with 4×10^5 $TCID_{50}$ HeV resulted in an average time to death of 8.5 days (Fig. 1). Clinical signs included decreased activity, piloerection of body hair, and mild depression as early as 5 days postinfection (p.i.) (Table 1). Rapidly progressive clinical illness was observed on day 7 or 9, with clinical signs including severe depression, severely reduced ability to move, and signs of respiratory disease (e.g., labored breathing, nasal discharge). According to a predetermined clinical endpoint scoring sheet and in consultation with a veterinarian, animals were euthanized when acute respiratory distress was obvious (as early as 7 days p.i.).

Treatment with ribavirin 24 h prior to or 12 h after challenge resulted in a significant delay in time to death (~2 days), whereas no effect was observed in animals treated 48 h p.i. (Fig. 1). Interestingly, the delay in death shifted the disease manifestations from primarily respiratory to neurological symptoms (Table 1). Neurological symptoms included muscle fasciculations of the arms and face as well as seizures progressively increasing in length, severity, and occurrence. The majority of animals started exhibiting neurological symptoms on day 9 p.i., which progressed until animals were euthanized based on a predetermined humane endpoint scoring sheet, although one animal showed neurological symptoms as early as day 7 p.i.

Blood biochemistry results included increased BUN and glucose levels and decreased albumin and total protein levels (data not shown).

Radiological and gross pathological changes. Respiratory disease development was analyzed by radiographic imaging (X ray), with the first signs of infiltration and interstitial markings in the lungs of some infected animals on day 7 p.i. (Fig. 2). This developed into diffuse interstitial infiltrates and cardiac border effacement with areas of pulmonary consolidation. Radiological changes were more severe in the control group and animals treated with ribavirin 48 h p.i.

Gross pathological changes observed during necropsies included sanguinous discharge from the nares (Fig. 3A) and severe lesions in the lungs, with affected lung lobes appearing plum colored, firm on palpation, and heavy and wet as signs for edema (Fig. 3B). Serous fluid was observed in the thoracic cavity in these animals. In agreement with the radiological changes, the percentage of affected lung lobes appeared larger in the control and 48-h treatment groups compared to the −24-h and 12-h treatment groups.

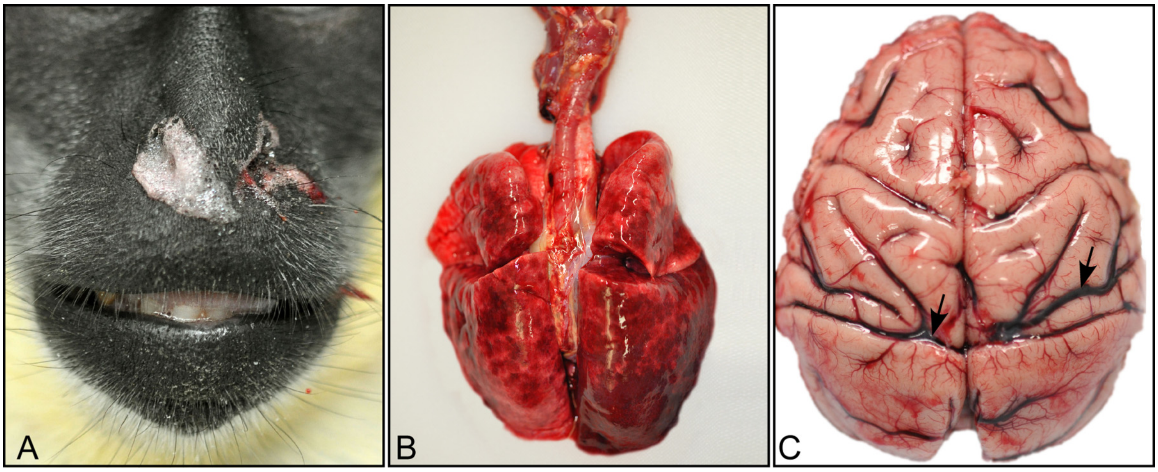

FIG. 3. Gross pathological changes observed during HeV infection of African green monkeys. Shown are gross pathological changes associated with the end stage of lethal HeV infection in African green monkeys. (A) Sanguinous froth exuding from nares; (B) enlarged lungs with multifocal areas of congestion and hemorrhage; (C) congestion of the brain (black arrows).

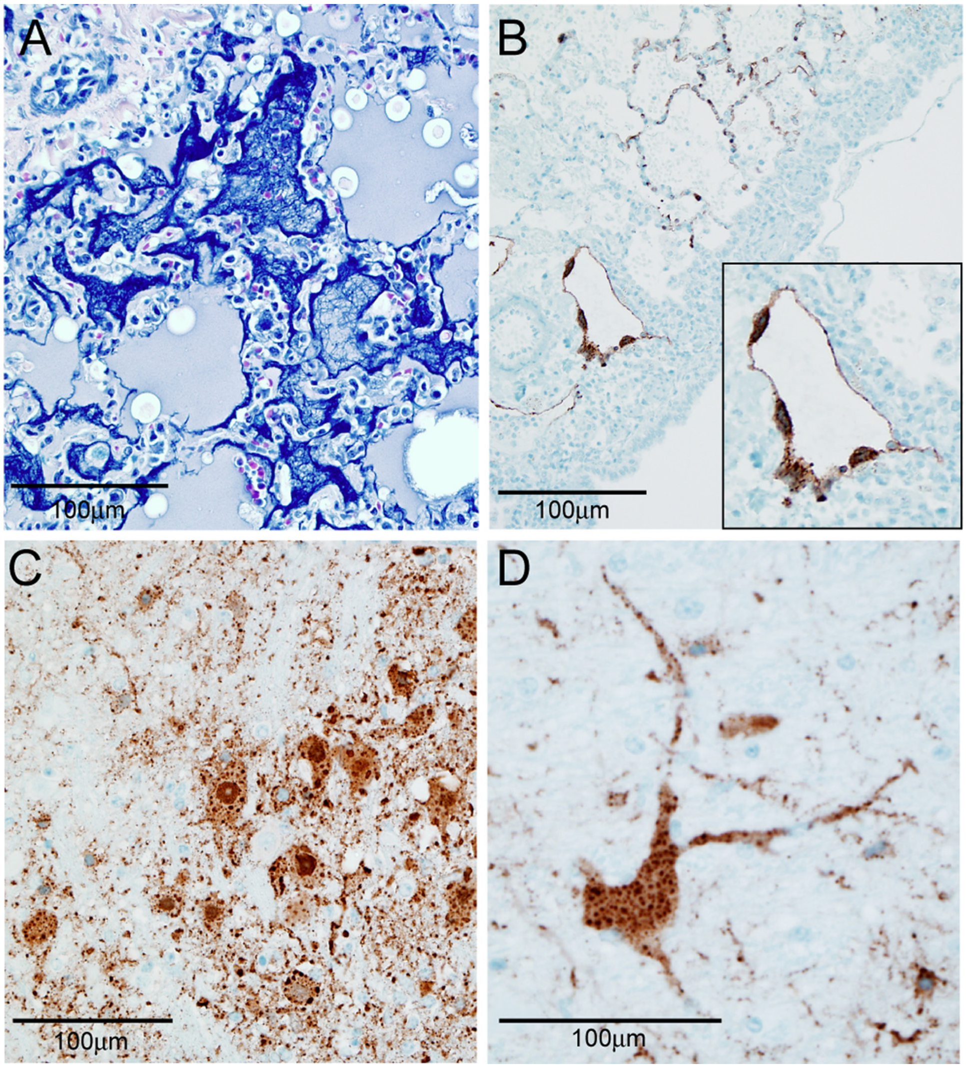

FIG. 4. Histological changes and tropism of HeV in tissues from infected African green monkeys. Shown are histological changes associated with the end stage of lethal HeV infection in African green monkeys (animal HeV1; Table 1). (A) Phosphotungstic acid-hematoxylin (PTAH) staining of lung lobe showing an abundance of polymerized fibrin in and around the alveolar spaces; (B) localization of HeV antigen by immunohistochemical (IHC) stain in the alveolar septae and within a lung blood vessel showing endothelial syncytia (inset); (C) IHC stain of HeV antigen in the brain stem; (D) detection of HeV antigen in neuron cell body and axon as well as surrounding cells.

Other gross pathological changes included enlarged cervical and bronchial lymph nodes, enlarged spleen, congested liver, and inflammation in the gastrointestinal tract (data not shown). In agreement with the observation of neurological symptoms, severe congestion of vessels in the brain was also present in several animals (Fig. 3C).

Histopathological changes in Hendra virus-infected African green monkeys. In agreement with the clinical presentation, radiological changes and gross pathological changes, intratracheal infection of AGM with HeV resulted in histopathology comparable to an acute respiratory distress syndrome (ARDS), including alveolar hemorrhaging, pulmonary edema, and inflammation. Injury to the gas exchange region in the lungs consisted of alveolitis, interstitial edema, and congestion in the alveolar septa and around small blood vessels. An abundance of polymerized fibrin was observed throughout the alveolar spaces (Fig. 4A). Endothelial syncytial cells were particularly prominent, and HeV antigen was primarily detected in the alveolar walls as well as the endothelium of small blood vessels (Fig. 4B). In the brain, HeV antigen was present in endothelial cells as well as in widespread areas of neurons (Fig. 4C and D). Interestingly, HeV antigen could be detected in the brain of animals with and without neurological symptoms.

Hendra virus replication in African green monkeys. To assess the dissemination and tissue tropism of HeV, infectious virus titers were determined in nasal, oral, and rectal swabs as well as in blood and a variety of tissues sampled at necropsy. In addition, these samples were also tested for presence of viral RNA by quantitative RT-PCR. Infectious virus could be recovered in a variety of tissues of control animals, including tissues throughout the respiratory tract, heart, liver, spleen, kidney, and a variety of lymph nodes (Fig. 5A). Interestingly, while ribavirin treatment did not protect against lethal HeV infection, virus titers and the number of tissues positive for

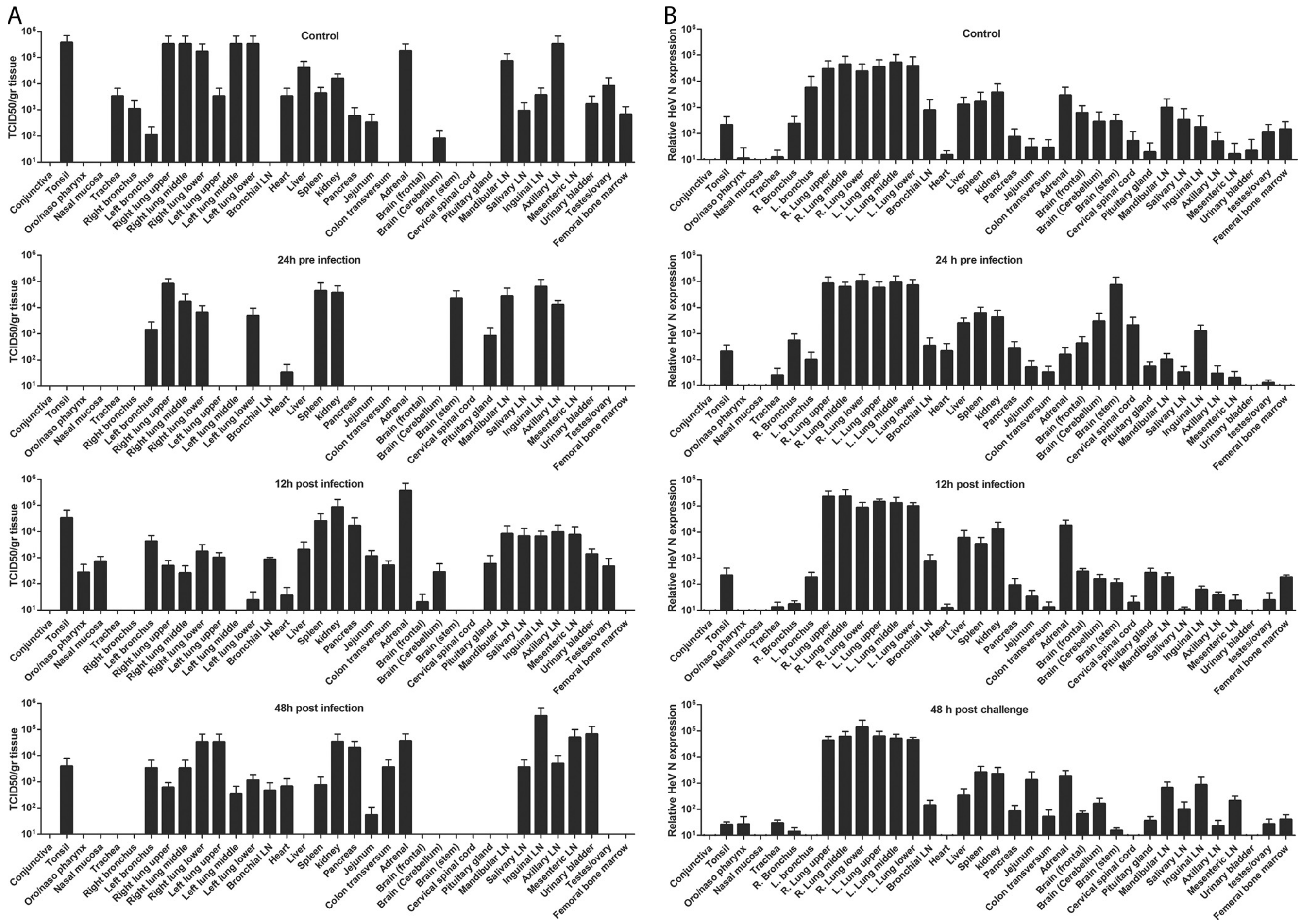

FIG. 5. Virus replication in tissues of HeV-infected African green monkeys. Virus replication was determined in tissues of HeV-infected animals by virus titration (A) and TaqMan RT-PCR (B) as described in Materials and Methods. For each treatment group, tissue samples from three animals were assayed and analyzed and the mean $TCID_{50}$ or relative HeV N expression values were calculated. The error bars represent the standard error of the mean. The $TCID_{50}$ titers are calculated per gram (gr) of tissue. LN, lymph node.

infectious virus were lower in animals treated 24 h prior to infection as compared to the controls. The primary tissues affected were the respiratory tract, spleen, kidney, brain stem, pituitary gland, and several lymph nodes. In addition, ribavirin treatment at 12 and 48 h postinfection also resulted in lower titers but not a reduction in the number of virus-positive tissues. While neurological symptoms were apparent in all ribavirin-treated groups, recovery of infectious virus from the central nervous system was variable and included infectious virus in the brain stem, pituitary gland, and cerebellum.

Low titers of infectious virus could also be detected in blood samples and oral, nasal, and rectal swabs of individual animals, but results were inconsistent with regard to treatment, samples and time postinfection (data not shown). Viral RNA was detectable in all organ tissues at variable levels (Fig. 5B). The highest relative viral RNA expression was detected in the lung tissue of infected animals, with no difference observed between the treatment groups. In addition, low levels of viral RNA were also detected in oral, nasal, rectal, and blood samples increasing over time (Fig. 6).

DISCUSSION

The henipaviruses are newly emerging zoonotic viruses that can cause severe respiratory illness and encephalitis in humans (14). Despite intensive studies, there are still no licensed vaccines or antiviral therapies for henipavirus infections. The goal of the present study was to develop a new NHP disease model to study the pathogenesis of lethal HeV infection and assess the efficacy of ribavirin as an antiviral treatment.

While several animals models have been described for both HeV and the related NiV, studies on pathogenesis and the development of effective therapeutics have been somewhat limited due to biocontainment restriction for work with the infectious pathogens and the absence of reagents for some animal species (25).

In the present study, we demonstrated that intratracheal inoculation of HeV in AGM results in a uniformly lethal infection within 7 to 9 days displaying largely as an acute respiratory distress syndrome (ARDS). The animals developed extensive diffuse interstitial infiltrates, as shown by radiological analysis, only 1 to 2 days prior to death. Upon necropsies,

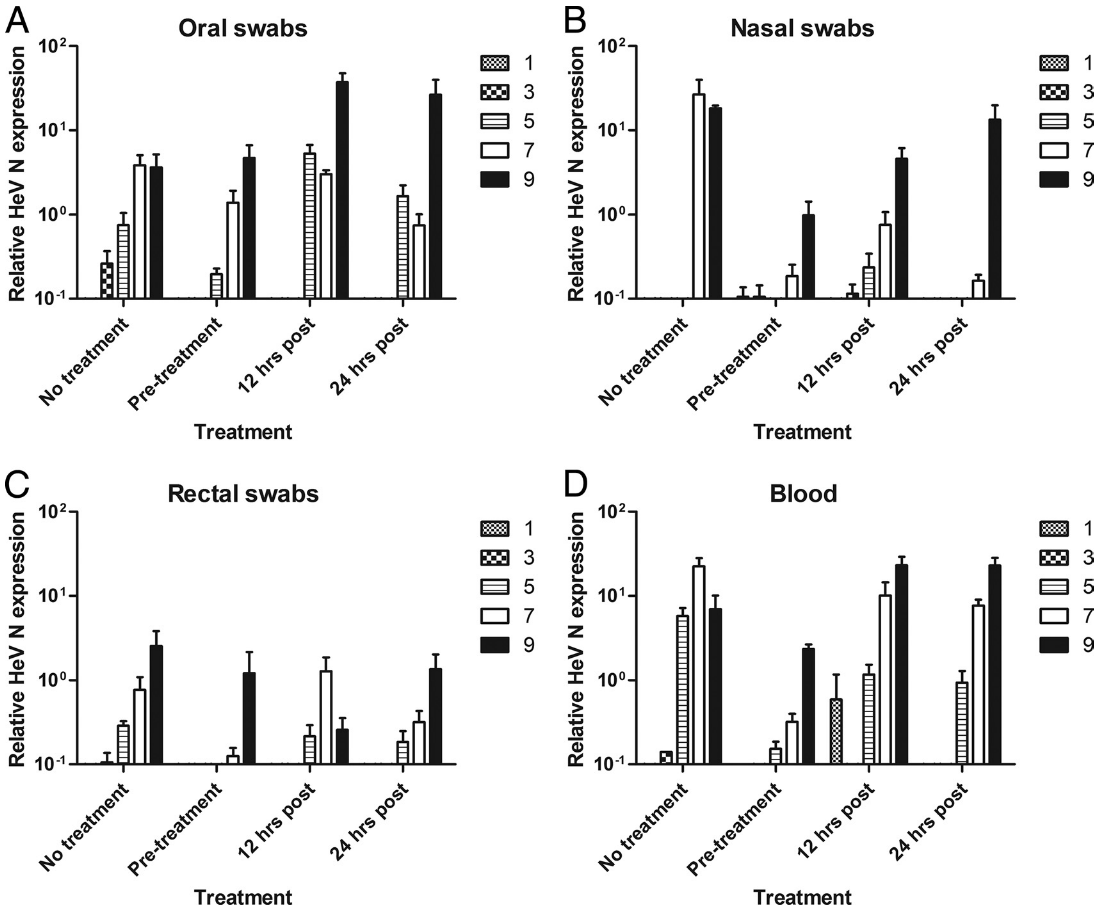

FIG. 6. Virus detection in samples from HeV-infected African green monkeys. TaqMan RT-PCR was used to determine the relative HeV N expression levels in oral (A), nasal (B), and rectal (C) swabs as well as in whole blood (D) on days 1, 3, 5, 7, and 9 postinfection. For each treatment group, samples from three animals were assayed and analyzed and the mean relative HeV N expression values were calculated. The error bars represent the standard error of the mean.

severe lung lesions were observed covering up to 90% of the tissue. Histopathological changes were primarily found in the lung and included alveolar hemorrhage, pulmonary edema, inflammation, and syncytial vascular endothelium, similar to what has been described in human cases of both HeV and NiV (27, 28). This is the first NHP disease model developed for HeV infection. Similar results were obtained when AGMs were infected with NiV (9), showing that this specific NHP species is a good and robust model for studying henipavirus infection. Recently NiV infection was described in squirrel monkeys (17). After intranasal or intravenous inoculation with NiV at high doses, several animals showed clinical signs, including acute respiratory distress and neurological symptoms; however, more than 50% of the animals either recovered or showed no symptoms. Although intravenous inoculation appeared more efficient than intranasal infection in establishing a symptomatic infection, NiV and HeV infection most likely occurs *per os* or through inhalation of contaminated fluids; thus, an intratracheal inoculation will be closer to the natural route of infection (12, 15, 16).

To date, only a limited number of human cases of HeV infection have been identified. Like in the AGM model, all human cases initially presented with ILI symptoms (22, 23, 27). In half of the cases, the disease progressed to neurological symptoms. During the outbreak of HeV in Australia in the summer of 2009, one individual died while receiving ribavirin treatment and three people with extensive exposure to the nasal secretions or blood of confirmed or highly suspected equine cases were admitted to hospital for a 5-day course of prophylaxis comprising intravenous ribavirin and oral chloroquine (ProMed-mail no. 20090826.2998). While these three people were released without developing any clinical symptoms after treatment, HeV infection was never confirmed. Therefore, whether ribavirin treatment is effective against HeV infection remains unknown.

The antiviral efficacy of ribavirin against henipaviruses has been shown in several *in vitro* studies; however, *in vivo* studies have had varied outcomes (1, 2, 8, 29). While ribavirin treatment in hamsters was not protective against lethal HeV challenge (8), an open-label ribavirin treatment trial run during an NiV outbreak in Malaysia in 1998 reported a reduction in mortality by 36% (6). Therefore, we used our newly developed AGM model to test the efficacy of ribavirin treatment against a lethal challenge with HeV.

Ribavirin treatment has been successfully used in a rhesus macaque model of Lassa virus infection (13). Using a similar therapeutic regiment, we treated three groups of three animals with ribavirin three times daily throughout the study, starting either 24 h prior to challenge or 12 or 48 h postchallenge. While none of the treatments protected against lethal HeV challenge, the 24-h pretreatments and 12-h posttreatments did significantly delay the time to death, similarly to what was seen in hamsters (8). In addition, the ribavirin treatment reduced the levels of viral replication, as seen in the Lassa virus model (13). Interestingly, the delay in time to death resulted in the development of neurological symptoms, including, among others, muscle fasciculations and seizures. The ribavirin treatment effectively lowered virus titers which apparently precluded the development of respiratory symptoms. The treatment did not seem to prevent systemic spread of the virus, and therefore infection of the central nervous system (CNS) could be established. As ribavirin does not cross the blood-brain barrier, no therapeutic benefit would be expected once CNS infection has occured. Similar results have been shown in Junin virus-infected rhesus monkeys, where ribavirin treatment increased the mean time to death and induced neurological symptoms (19, 26).

While neurological symptoms were not seen in HeV-infected control AGMs, these animals succumbed to an acute onset of respiratory distress before virus-associated clinical symptoms from infection of the central nervous system became obvious. By lowering the viral dose through ribavirin treatment systemically, respiratory symptoms are less pronounced, but spread to the CNS is not affected, resulting in the appearance of neurological symptoms. Similar results were observed in hamsters and ferrets, where a low dose of NiV or HeV resulted in a longer mean time to death and more neurological symptoms, whereas a high dose resulted in the rapid development of severe respiratory distress (unpublished data). Therefore, lowering but not clearing HeV systemically will result in the development of both respiratory and neurological symptoms, with the neurological symptoms becoming more pronounced.

Based on the data here, ribavirin treatment does not seem to be effective against lethal HeV infection. While there are currently no approved treatments, several treatment and vaccine candidates have been evaluated using rodent, cat, and ferret models. The most successful treatment strategy reported to date makes use of the cross-neutralizing, fully human monoclonal antibody m102.4 (5, 30). This passive antibody treatment proved fully protective when a single dose was administered 10 h postchallenge in a ferret model of lethal NiV infection. In addition, a vaccination boost strategy using a recombinant soluble attachment glycoprotein (sG) from either HeV or NiV has shown protective efficacy against lethal NiV challenge in cats (18, 20). Both of these intervention strategies are currently being evaluated using the recently developed AGM models for lethal HeV and NiV infection.

In conclusion, our data show that AGMs can be efficiently infected with HeV and the disease progression closely mirrors that seen in human cases. We believe that this new model will be a powerful tool for studying the pathogenesis of HeV infection as well as an essential model for the development of vaccines and therapeutics in the future. This study demonstrated that ribavirin can delay clinical progression of HeV infection but does not prevent lethal outcome. Therefore, we propose that ribavirin is of limited efficacy for HeV infection, and given the sometimes severe side affects associated with ribavirin and the potential for developing an encephalitic syndrome, it may not be recommended as a single therapy for HeV infections. Efficacy may increase in combination therapy with other treatment modalities such as drugs or antibodies (4, 5). However, this remains to be investigated before recommendations can be made.

ACKNOWLEDGMENTS

We thank Edward Schreckendgust, Rocky Rivera, Sandy Skorupa, Kathleen Meuchel, Don Gardner, Rachel LaCasse, and Michael Parnell (Rocky Mountain Veterinary Branch [RMVB], Division of Intramural Research [DIR], National Institute of Allergy and Infectious Diseases [NIAID], National Institutes of Health [NIH]) for assistance with animal care and animal procedures; Anita Mora (DIR, NIAID, NIH) for assistance with graphical work; and Rebecca Rosenke (RMVB, DIR, NIAID, NIH) for technical assistance with aspects of histopathology.

This study was supported in part by the Department of Health and Human Services, NIH, grants AI082121 and AI057159 to Thomas W. Geisbert and funding from DIR, NIAID, NIH, to the Laboratory of Virology.

The authors declare they have no conflicts of interest.

REFERENCES

1. **Aljofan, M., M. Porotto, A. Moscona, and B. A. Mungall.** 2008. Development and validation of a chemiluminescent immunodetection assay amenable to high throughput screening of antiviral drugs for Nipah and Hendra virus. J. Virol. Methods **149:**12–19.
2. **Aljofan, M., S. Saubern, A. G. Meyer, G. Marsh, J. Meers, and B. A. Mungall.** 2009. Characteristics of Nipah virus and Hendra virus replication in different cell lines and their suitability for antiviral screening. Virus Res. **142:**92–99.
3. **Bishop, K. A., and C. C. Broder.** 2008. Hendra and Nipah: lethal zoonotic paramyxoviruses. American Society for Microbiology, Washington, DC.
4. **Bossart, K. N., B. A. Mungall, G. Crameri, L. F. Wang, B. T. Eaton, and C. C. Broder.** 2005. Inhibition of Henipavirus fusion and infection by heptad-derived peptides of the Nipah virus fusion glycoprotein. Virol. J. **2:**57.
5. **Bossart, K. N., Z. Zhu, D. Middleton, J. Klippel, G. Crameri, J. Bingham, J. A. McEachern, D. Green, T. J. Hancock, Y. P. Chan, A. C. Hickey, D. S. Dimitrov, L. F. Wang, and C. C. Broder.** 2009. A neutralizing human monoclonal antibody protects against lethal disease in a new ferret model of acute nipah virus infection. PLoS Pathog. **5:**e1000642.
6. **Chong, H. T., A. Kamarulzaman, C. T. Tan, K. J. Goh, T. Thayaparan, S. R. Kunjapan, N. K. Chew, K. B. Chua, and S. K. Lam.** 2001. Treatment of acute Nipah encephalitis with ribavirin. Ann. Neurol. **49:**810–813.
7. **Chua, K. B., K. J. Goh, K. T. Wong, A. Kamarulzaman, P. S. Tan, T. G. Ksiazek, S. R. Zaki, G. Paul, S. K. Lam, and C. T. Tan.** 1999. Fatal encephalitis due to Nipah virus among pig-farmers in Malaysia. Lancet **354:**1257–1259.
8. **Freiberg, A. N., M. N. Worthy, B. Lee, and M. R. Holbrook.** 2010. Combined chloroquine and ribavirin treatment does not prevent death in a hamster model of Nipah and Hendra virus infection. J. Gen. Virol. **91:**765–772.
9. **Geisbert, T. W., K. M. Daddario-Dicaprio, A. C. Hickey, M. A. Smith, Y. P. Chan, L. F. Wang, J. J. Mattapallil, J. B. Geisbert, K. N. Bossart, and C. C. Broder.** 2010. Development of an acute and highly pathogenic nonhuman primate model of nipah virus infection. PLoS One **5:**e10690.
10. **Georges-Courbot, M. C., H. Contamin, C. Faure, P. Loth, S. Baize, P. Leyssen, J. Neyts, and V. Deubel.** 2006. Poly(I)-poly(C_{12}U) but not ribavirin prevents death in a hamster model of Nipah virus infection. Antimicrob. Agents Chemother. **50:**1768–1772.
11. **Guillaume, V., K. T. Wong, R. Y. Looi, M. C. Georges-Courbot, L. Barrot, R. Buckland, T. F. Wild, and B. Horvat.** 2009. Acute Hendra virus infection: analysis of the pathogenesis and passive antibody protection in the hamster model. Virology **387:**459–465.
12. **Gurley, E. S., J. M. Montgomery, M. J. Hossain, M. Bell, A. K. Azad, M. R. Islam, M. A. Molla, D. S. Carroll, T. G. Ksiazek, P. A. Rota, L. Lowe, J. A. Comer, P. Rollin, M. Czub, A. Grolla, H. Feldmann, S. P. Luby, J. L. Woodward, and R. F. Breiman.** 2007. Person-to-person transmission of Nipah virus in a Bangladeshi community. Emerg. Infect. Dis. **13:**1031–1037.
13. **Jahrling, P. B., R. A. Hesse, G. A. Eddy, K. M. Johnson, R. T. Callis, and E. L. Stephen.** 1980. Lassa virus infection of rhesus monkeys: pathogenesis and treatment with ribavirin. J. Infect. Dis. **141:**580–589.
14. **Lo, M. K., and P. A. Rota.** 2008. The emergence of Nipah virus, a highly pathogenic paramyxovirus. J. Clin. Virol. **43:**396–400.
15. **Looi, L. M., and K. B. Chua.** 2007. Lessons from the Nipah virus outbreak in Malaysia. Malays. J. Pathol. **29:**63–67.

16. **Luby, S. P., E. S. Gurley, and M. J. Hossain.** 2009. Transmission of human infection with Nipah virus. Clin. Infect. Dis. **49:**1743–1748.
17. **Marianneau, P., V. Guillaume, T. Wong, M. Badmanathan, R. Y. Looi, S. Murri, P. Loth, N. Tordo, F. Wild, B. Horvat, and H. Contamin.** 2010. Experimental infection of squirrel monkeys with nipah virus. Emerg. Infect. Dis. **16:**507–510.
18. **McEachern, J. A., J. Bingham, G. Crameri, D. J. Green, T. J. Hancock, D. Middleton, Y. R. Feng, C. C. Broder, L. F. Wang, and K. N. Bossart.** 2008. A recombinant subunit vaccine formulation protects against lethal Nipah virus challenge in cats. Vaccine **26:**3842–3852.
19. **McKee, K. T., Jr., J. W. Huggins, C. J. Trahan, and B. G. Mahlandt.** 1988. Ribavirin prophylaxis and therapy for experimental Argentine hemorrhagic fever. Antimicrob. Agents Chemother. **32:**1304–1309.
20. **Mungall, B. A., D. Middleton, G. Crameri, J. Bingham, K. Halpin, G. Russell, D. Green, J. McEachern, L. I. Pritchard, B. T. Eaton, L. F. Wang, K. N. Bossart, and C. C. Broder.** 2006. Feline model of acute Nipah virus infection and protection with a soluble glycoprotein-based subunit vaccine. J. Virol. **80:**12293–12302.
21. **O'Sullivan, J. D., A. M. Allworth, D. L. Paterson, T. M. Snow, R. Boots, L. J. Gleeson, A. R. Gould, A. D. Hyatt, and J. Bradfield.** 1997. Fatal encephalitis due to novel paramyxovirus transmitted from horses. Lancet **349:**93–95.
22. **Playford, E. G., B. McCall, G. Smith, V. Slinko, G. Allen, I. Smith, F. Moore, C. Taylor, Y. H. Kung, and H. Field.** 2010. Human Hendra virus encephalitis associated with equine outbreak, Australia, 2008. Emerg. Infect. Dis. **16:**219–223.
23. **Selvey, L. A., R. M. Wells, J. G. McCormack, A. J. Ansford, K. Murray, R. J. Rogers, P. S. Lavercombe, P. Selleck, and J. W. Sheridan.** 1995. Infection of humans and horses by a newly described morbillivirus. Med. J. Aust. **162:** 642–645.
24. **Snoy, P. J.** 15 June 2010, posting date. Establishing efficacy of human products using animals: the US Food and Drug Administration's "Animal Rule." Vet. Pathol. [Epub ahead of print.]
25. **Weingartl, H. M., Y. Berhane, and M. Czub.** 2009. Animal models of henipavirus infection: a review. Vet. J. **181:**211–220.
26. **Weissenbacher, M. C., M. A. Calello, M. S. Merani, J. B. McCormick, and M. Rodriguez.** 1986. Therapeutic effect of the antiviral agent ribavirin in Junin virus infection of primates. J. Med. Virol. **20:**261–267.
27. **Wong, K. T., T. Robertson, B. B. Ong, J. W. Chong, K. C. Yaiw, L. F. Wang, A. J. Ansford, and A. Tannenberg.** 2009. Human Hendra virus infection causes acute and relapsing encephalitis. Neuropathol. Appl. Neurobiol. **35:** 296–305.
28. **Wong, K. T., W. J. Shieh, S. Kumar, K. Norain, W. Abdullah, J. Guarner, C. S. Goldsmith, K. B. Chua, S. K. Lam, C. T. Tan, K. J. Goh, H. T. Chong, R. Jusoh, P. E. Rollin, T. G. Ksiazek, and S. R. Zaki.** 2002. Nipah virus infection: pathology and pathogenesis of an emerging paramyxoviral zoonosis. Am. J. Pathol. **161:**2153–2167.
29. **Wright, P. J., G. Crameri, and B. T. Eaton.** 2005. RNA synthesis during infection by Hendra virus: an examination by quantitative real-time PCR of RNA accumulation, the effect of ribavirin and the attenuation of transcription. Arch. Virol. **150:**521–532.
30. **Zhu, Z., K. N. Bossart, K. A. Bishop, G. Crameri, A. S. Dimitrov, J. A. McEachern, Y. Feng, D. Middleton, L. F. Wang, C. C. Broder, and D. S. Dimitrov.** 2008. Exceptionally potent cross-reactive neutralization of Nipah and Hendra viruses by a human monoclonal antibody. J. Infect. Dis. **197:** 846–853.